by action of π ligands, which are without effect on it.

The reactions are summarized as follows:

$$[(\text{triphos})\text{Co}(\mu\text{-SCH}_3)_2\text{Co}(\text{triphos})]^{2+}$$
$$\xrightarrow{\text{CO}} 2[(\text{triphos})\text{Co}(\text{CO})(\text{SCH}_3)]^+$$
$$\xrightarrow{\text{NaBH}_4} 2[(\text{triphos})\text{Co}(\text{SCH}_3)]$$
$$\xrightarrow{\text{NOBF}_4} \text{decomposition}$$

$$[(\text{triphos})\text{Co}(\mu\text{-S})_2\text{Co}(\text{triphos})]^+$$
$$\xrightarrow{\text{CO}} \text{no reaction}$$
$$\xrightarrow{\text{NaBH}_4} [(\text{triphos})\text{Co}(\mu\text{-S})_2\text{Co}(\text{triphos})]$$
$$\xrightarrow{\text{NOBF}_4} [(\text{triphos})\text{Co}(\mu\text{-S})_2\text{Co}(\text{triphos})]^{2+}$$

The complexes $[(\text{triphos})\text{Co}(\text{SCH}_3)]$ and $[(\text{triphos})\text{Co}(\text{CO})(\text{SCH}_3)]\text{BPh}_4$ are isostructural with both the pseudotetrahedral complexes[18] $[(\text{triphos})\text{CoX}]$ (X = Cl, Br, I) and the five-coordinated complexes[19] $[(\text{triphos})\text{Co}(\text{CO})\text{X}]\text{BPh}_4$ (X = Cl, Br), respectively. The latter five-coordinate complexes are obtained from $[(\text{triphos})_2\text{Co}_2\text{X}_2]^{2+}$ (X = Cl, Br) by reactions analogous to the above ones.

Acknowledgment. Thanks are expressed to Mr. F. Cecconi for technical assistance and to Mr. F. Nuzzi and Mr. G. Vignozzi for microanalyses.

Registry No. **1**, 73496-93-2; **2**, 73697-77-5; **3**, 73496-94-3; $[(\text{triphos})_2\text{Co}_2\text{S}_2](\text{BPh}_4)_2$, 73496-96-5; $[(\text{triphos})\text{Co}(\text{CO})(\text{SCH}_3)]\text{BPh}_4$, 73496-98-7; $(\text{triphos})\text{Co}(\text{SCH}_3)$, 73496-99-8; $[(\text{triphos})_2\text{Co}_2(\mu\text{-OH})_2](\text{BPh}_4)_2$, 56172-82-8.

Supplementary Material Available: Listings of structure factor amplitudes for compounds **1**–**3** (45 pages). Ordering information is given on any current masthead page.

---

(18) (a) Sacconi, L.; Midollini, S. *J. Chem. Soc., Dalton Trans.* **1972**, 1213. (b) Dapporto, P.; Fallani, G.; Midollini, S.; Sacconi, L. *J. Chem. Soc., Chem. Commun.* **1972**, 1161.

(19) Ghilardi, C. A.; Midollini, S.; Sacconi, L. *J. Organomet. Chem.* **1980**, *186*, 279.

Contribution No. 6067 from the Arthur Amos Noyes Laboratory of Chemical Physics,
California Institute of Technology, Pasadena, California 91125

Crystal Structure Analyses of $\text{Rh}_2(\text{bridge})_4(\text{BPh}_4)_2\cdot\text{CH}_3\text{CN}$ and $\text{Rh}_2(\text{TM4-bridge})_4(\text{PF}_6)_2\cdot2\text{CH}_3\text{CN}$. Further Electronic Spectral Studies of Binuclear Rhodium(I) Isocyanide Complexes

KENT R. MANN, JOHN A. THICH, ROBERT A. BELL, CATHERINE L. COYLE, and HARRY B. GRAY*

Received July 12, 1979

We have performed X-ray crystal structure analyses of $\text{Rh}_2(\text{bridge})_4(\text{BPh}_4)_2\cdot\text{CH}_3\text{CN}$ (bridge = 1,3-diisocyanopropane) (space group $P2_1/m$; C_{2h}^2; No. 11; $Z = 2$; $a = 17.359$ (6), $b = 12.573$ (4), $c = 15.666$ (8) Å; $\beta = 113.08$ (3)°; d(calcd) = 0.332 (1), d(obsd) = 1.31 (1) g/cm^3) and $\text{Rh}_2(\text{TM4-bridge})_4(\text{PF}_6)_2\cdot2\text{CH}_3\text{CN}$ (TM4-bridge = 2,5-dimethyl-2,5-diisocyanohexane) (space group $P4_2/mbc$; No. 135; $Z = 4$; $a = b = 14.690$ (1), $c = 29.370$ (1) Å; d(calcd) = 1.294 (1), d(obsd) = 1.29 (1) g/cm^3). $\text{Rh}_2(\text{bridge})_4(\text{BPh}_4)_2\cdot\text{CH}_3\text{CN}$ contains ligand-bridged binuclear cations. The ligands are rigorously eclipsed in $\text{Rh}_2(\text{bridge})_4{}^{2+}$, and the coordination geometry about the Rh atoms is essentially square planar, with a Rh–Rh distance of 3.242 (1) Å. $\text{Rh}_2(\text{TM4-bridge})_4(\text{PF}_6)_2\cdot2\text{CH}_3\text{CN}$ also contains discrete ligand-bridged binuclear cations. Although each Rh unit again exhibits approximately square-planar geometry, the rotameric ligand conformation is partially staggered (an angle of about 30° from eclipsed). The Rh–Rh distance is 3.262 (1) Å, which is slightly longer than that in $\text{Rh}_2(\text{bridge})_4{}^{2+}$. The absorption and emission spectra of several binuclear rhodium(I) isocyanide complexes have been measured in acetonitrile solution at room temperature. All the complexes exhibit an intense low-energy absorption spectral band between 400 and 600 nm that is attributable to the fully allowed ${}^1\text{A}_{1g} \rightarrow {}^1\text{A}_{2u}$ transition. Relatively strong emission attributable to ${}^1\text{A}_{2u} \rightarrow {}^1\text{A}_{1g}$ is also observed in the 600–700-nm region; the Stokes shift of the emission band is a function of the rotameric conformation of the CNR groups in the binuclear Rh(I) complexes, the order being CNPhCH_3 (staggered) > TM4-bridge (partially staggered) > bridge (eclipsed).

The work reported in this paper grew out of studies of the spectroscopic properties of rhodium(I) isocyanides, which we initiated in 1973. One discovery we made early in these studies was that $\text{Rh}(\text{CNR})_4{}^+$ complexes aggregate in solution, yielding discrete binuclear, trinuclear, and even higher oligomers.[1,2] We became intrigued with the spectroscopic properties of these oligomeric Rh(I) species and decided to prepare a particular binuclear complex, $\text{Rh}_2(\text{bridge})_4{}^{2+}$ (bridge = 1,3-diisocyanopropane), for detailed study.[3] The spectroscopic properties, the thermal redox chemistry, and particularly the photoredox chemistry of $\text{Rh}_2(\text{bridge})_4{}^{2+}$ and its derivatives turned out to be interesting,[3-8] and we are continuing our investigations of this system.

---

(1) Mann, K. R.; Gordon, J. G., II; Gray, H. B. *J. Am. Chem. Soc.* **1975**, *97*, 3553.

(2) Mann, K. R.; Lewis, N. W.; Williams, R. M.; Gray, H. B.; Gordon, J. G., II *Inorg. Chem.* **1978**, *17*, 828.

(3) Lewis, N. S.; Mann, K. R.; Gordon, J. G., II; Gray, H. B. *J. Am. Chem. Soc.* **1976**, *98*, 746.

(4) Mann, K. R.; Lewis, N. S.; Miskowski, V. M.; Erwin, D. K.; Hammond, G. S.; Gray, H. B. *J. Am. Chem. Soc.* **1977**, *99*, 5525.

(5) Miskowski, V. M.; Nobinger, G. L.; Kliger, D. S.; Hammond, G. S.; Lewis, N. S.; Mann, K. R.; Gray, H. B. *J. Am. Chem. Soc.* **1978**, *100*, 485.

(6) (a) Gray, H. B.; Mann, K. R.; Lewis, N. S.; Thich, J. A.; Richman, R. M. *Adv. Chem. Ser.* **1978**, *No. 168*, 44. (b) Mann, K. R.; Gray, H. B. *Ibid.* **1979**, *No. 173*, 255.

(7) (a) Miskowski, V. M.; Sigal, I. S.; Mann, K. R.; Gray, H. B.; Milder, S. J.; Hammond, G. S.; Ryason, P. R. *J. Am. Chem. Soc.* **1979**, *101*, 4383. (b) Sigal, I. S.; Mann, K. R.; Gray, H. B., to be submitted for publication. (c) Sigal, I. S.; Gray, H. B., to be submitted for publication.

(8) Mann, K. R.; Bell, R. A.; Gray, H. B. *Inorg. Chem.* **1979**, *18*, 2671.

0020-1669/80/1319-2462$01.00/0

Table I. Crystal Data

$Rh_2(bridge)_4(BPh_4)_2 \cdot CH_3CN$

fw 1261.8	$V = 3145$ (2) Å^3
space group $P2_1/m$ ($C_{2h}{}^2$, No. 11)	d(calcd) = 1.332 g/cm^3
$a = 17.359$ (6) Å	d(obsd) = 1.31 (1) g/cm^3
$b = 12.573$ (4) Å	$\lambda = 0.710\,69$ Å
$c = 15.666$ (8) Å	temp = 22 (1) °C
$\beta = 113.08$ (3)°	$\mu = 5.62$ cm^{-1} for Mo Kα
$Z = 2$	

$Rh_2(TM4\text{-}bridge)_4(PF_6)_2 \cdot 2CH_3CN$

fw 1234.9	$V = 6338$ (3) Å^3
space group $P4_2/mbc$ (No. 135)	d(calcd) = 1.294 (1) g/cm^3
$a = 14.690$ (1) Å	d(obsd) = 1.29 (3) g/cm^3
$c = 29.370$ (1) Å	$\lambda = 0.710\,69$ Å
$Z = 4$	temp = 22 (1) °C
	$\mu = 6.26$ cm^{-1} for Mo Kα

One particularly striking feature in the electronic absorption spectrum of $Rh_2(bridge)_4{}^{2+}$ is an intense, low-lying band (λ_{max} = 553 nm in CH_3CN solution). We have assigned this band to $^1A_{1g} \rightarrow {}^1A_{2u}$ ($1a_{2u} \rightarrow 2a_{1g}$ ($p_z,\pi^*(CNR)$)), a transition involving axially directed donor and acceptor orbitals, with the latter having ligand π^* character as well.[3] The energy of this transition should be a sensitive function of both the metal–metal and the ligand–ligand interactions. To test this prediction, we have prepared two additional binuclear Rh(I) complexes, $Rh_2(4\text{-bridge})_4{}^{2+}$ (4-bridge = 1,4-diisocyanobutane) and $Rh_2(TM4\text{-bridge})_4{}^{2+}$ (TM4-bridge = 2,5-dimethyl-2,5-diisocyanohexane), and have studied their spectroscopic properties. Interpretation of these results has been facilitated by two X-ray crystal structure determinations, those of $Rh_2(bridge)_4(BPh_4)_2 \cdot CH_3CN$ and $Rh_2(TM4\text{-}bridge)_4(PF_6)_2 \cdot 2CH_3CN$.

Experimental Section

Standard procedures were used to prepare 1,3-diisocyanopropane (bridge) and $Rh_2(bridge)_4(BPh_4)_2 \cdot CH_3CN$.[3] Absorption[2] and emission[5] spectra were measured as described previously.

2,5-Dimethyl-2,5-diisocyanohexane (TM4-bridge). TM4-bridge was prepared from the corresponding amine by the method of Weber et al.[9] and recrystallized from CH_2Cl_2. $\bar{\nu}$(CN) 2126 cm^{-1} (CH_2Cl_2 solution); NMR triplet (CH_3) τ 8.5 (Me_4Si reference), broad singlet (CH_2) τ 8.2, 3:1 ratio ($CDCl_3$ solution).

1,4-Diisocyanobutane (4-bridge). 4-bridge was prepared from the corresponding amine by a standard method[9] and purified by vacuum distillation. $\bar{\nu}$(CN) 2145 cm^{-1} (neat).

$Rh_2(TM4\text{-}bridge)_4(PF_6)_2$. $AgPF_6$ (0.630 g, 2.5 mmol) was added to 25 mL of a stirred acetonitrile solution containing $[Rh(COD)Cl]_2$ (0.616 g, 1.25 mmol) (the latter compound was prepared by a standard method[10]). The AgCl precipitate was filtered off and then TM4-bridge (0.822 g, 5 mmol) was added to the light yellow filtrate. The solution immediately turned dark maroon. Diethyl ether was added and the resulting precipitate was recrystallized from acetonitrile/ether and air-dried. Yields were about 80% of recrystallized product. Anal. Calcd for $Rh_2(TM4\text{-}bridge)_4(PF_6)_2$: C, 41.68; H, 5.60; N, 9.72. Found: C, 41.38; H, 5.47; N, 10.08. ν(CN) 2152 cm^{-1} (CH_2Cl_2 solution).

$Rh_2(4\text{-bridge})_4(BPh_4)_2$. 4-bridge (1.1 g) was dissolved in 100 mL of $CHCl_3$. Ten milliliters of this solution was added to 50 mL of CH_3CN in an Erlenmeyer flask. The resulting solution was purged with nitrogen for 5 min. $Rh_2(CO)_4Cl_2$ (0.10 g)[11] in 5 mL of $CHCl_3$ was then added dropwise to the 4-bridge while maintaining vigorous stirring and a nitrogen blanket. After complete addition, the solution was deep red-purple, and some precipitation had occurred. Stirring was maintained for 5 min more and an equal volume of diethyl ether was added to precipitate all solids. The resulting dull blue-gray powder was washed with $CHCl_3$ and ether and dried under a stream of N_2. The blue-gray powder was extracted with methanol several times. Solid $NaBPh_4$ (excess) was added to the filtrate. A navy blue product precipitated immediately. This was isolated by filtration and washed with water, methanol, and ether. The product was air-dried. Yields were in general poor (less than 30% based on $Rh_2(CO)_4Cl_2$) and variable. The complex obtained in this fashion was purified by reprecipitation from CH_3CN/ether mixtures. Anal. Calcd for $Rh_2(4\text{-bridge})_4(BPh_4)_2$: C, 67.73; H, 5.68; N, 8.78. Found: C, 66.75; H, 5.65; N, 8.99. ν(CN) 2170 cm^{-1} (KBr pellet).

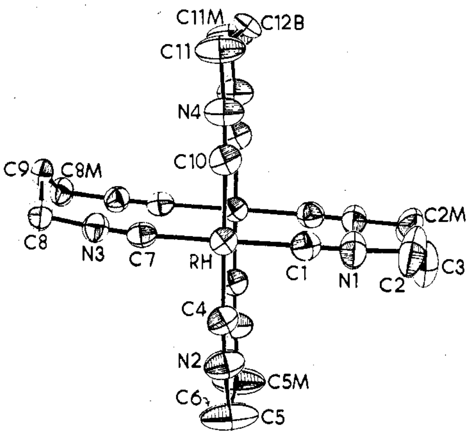

Figure 1. View of the structure of $Rh_2(bridge)_4{}^{2+}$.

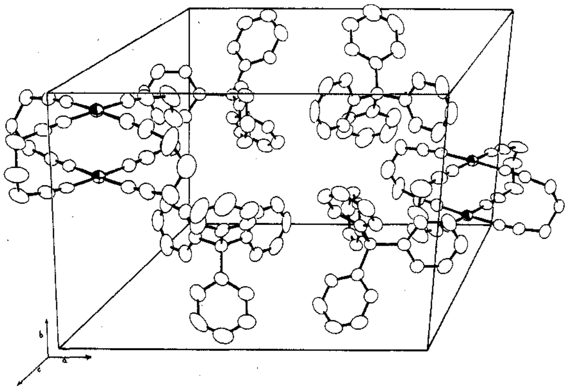

Figure 2. View of the unit cell of $Rh_2(bridge)_4(BPh_4)_2 \cdot CH_3CN$ perpendicular to the Rh–Rh axis.

Collection and Reduction of Diffraction Data for $Rh_2(bridge)_4(BPh_4)_2 \cdot CH_3CN$. Blue-black parallelepipeds of $Rh_2(bridge)_4(BPh_4)_2$ were obtained by slow evaporation (~3 months) of a cooled acetonitrile solution. A crystal of approximate dimensions 0.8 × 0.2 × 0.2 mm was mounted on the tip of a glass fiber along its long dimension (b axis). Preliminary Weissenberg and precession photographs revealed monoclinic symmetry with systematic absences $0k0$, $k = 2n + 1$. These absences are consistent with space groups $P2_1$ and $P2_1/m$. Successful solution and refinement of the structure confirmed the latter as the correct choice. Unit cell constants (Table I), determined at room temperature by using a Syntex $P2_1$ diffractometer and Mo Kα radiation, were obtained from a least-squares fit on the basis of 15 moderately intense reflections. The density was measured by flotation in a mixture of chloroform and hexane. The observed density of 1.31 (1) g/cm^3 agrees satisfactorily with the value of 1.332 (1) g/cm^3 calculated for two formula units per unit cell.

Intensity data were collected at 22 °C by using monochromatized (graphite, $\theta = 6.08$) Mo Kα radiation. A θ–2θ scan was used, and data out to $2\theta = 60°$ were collected. Each scan covered a range from 1° below Kα_1 to 1° above Kα_2 for the calculated peak position. All data were collected by using a scan rate of 2.02° min^{-1} with stationary background counts taken before and after each scan. The total time for background counts equaled the scan time and was equally distributed before and after the peak. Two standard reflections were collected at intervals of 30 reflections throughout the data collection. No significant trends, decay, or fluctuations (±2% max) were observed in the intensities of either check reflection. Of a total of 11 319 reflections collected, the 4589 with $F^2 > 3\sigma(F^2)$ were used in the solution and refinement of the structure. Observational variances,

---

(9) Weber, W. P.; Gobel, G. W.; Ugi, I. K. *Angew Chem., Int. Ed. Engl.* **1972**, *11*, 530.

(10) Chatt, J.; Venanzi, L. M. *J. Chem. Soc.* **1957**, 4735.

(11) McCleverty, J. A.; Wilkinson, G. *Inorg. Synth.* **1966**, *8*, 211.

Table II. Final Atom Parameters (Coordinates $\times 10^5$, $U_{ij} \times 10^4$)[a, b] for $Rh_2(bridge)_4(BPh_4)_2 \cdot CH_3CN$

atom	x	y	z	U_{11}	U_{22}	U_{33}	U_{12}	U_{13}	U_{23}
Rh	−5 975 (3)	12 108 (3)	14 798 (3)	452 (2)	344 (2)	473 (2)	−15 (3)	189 (2)	−32 (2)
C1	−17 555 (31)	12 566 (43)	5 652 (31)	537 (32)	490 (28)	511 (30)	−66 (34)	222 (27)	−60 (29)
N1	−24 307 (26)	13 237 (39)	673 (28)	459 (27)	787 (34)	575 (27)	92 (31)	88 (23)	−135 (28)
C2	−32 675 (36)	15 049 (65)	−5 951 (45)	425 (36)	1501 (76)	1083 (52)	−2 (44)	119 (37)	−751 (53)
C3	−36 166 (60)	25 000 (0)	−4 486 (71)	557 (68)	1531 (111)	943 (80)	0 (0)	−52 (60)	0 (0)
C4	−10 361 (30)	12 269 (42)	24 574 (33)	541 (32)	397 (25)	617 (31)	−79 (31)	274 (27)	−78 (29)
N2	−13 094 (30)	13 030 (38)	30 112 (31)	892 (37)	622 (30)	839 (34)	−149 (33)	576 (31)	−163 (30)
C5	−17 050 (53)	14 952 (56)	36 616 (50)	1811 (81)	853 (54)	1339 (59)	−285 (54)	1304 (63)	−177 (48)
C6	−16 881 (76)	25 000 (0)	39 849 (79)	1645 (117)	916 (75)	1558 (100)	0 (0)	1413 (98)	0 (0)
C7	5 757 (30)	12 272 (40)	23 901 (30)	532 (31)	382 (24)	516 (28)	−15 (32)	279 (26)	15 (27)
N3	12 656 (24)	13 022 (32)	28 849 (24)	442 (24)	468 (24)	511 (24)	50 (26)	173 (21)	3 (23)
C8	21 356 (30)	14 854 (40)	34 623 (32)	396 (29)	589 (36)	501 (30)	64 (27)	97 (25)	−7 (26)
C9	24 460 (42)	25 000 (0)	31 830 (45)	322 (41)	609 (46)	412 (40)	0 (0)	107 (35)	0 (0)
C10	−1 658 (30)	12 504 (39)	4 969 (32)	596 (34)	277 (22)	637 (32)	−25 (30)	277 (28)	−1 (29)
N4	1 185 (28)	13 316 (32)	−484 (29)	871 (35)	308 (21)	718 (29)	−19 (25)	493 (27)	−9 (23)
C11	5 132 (43)	15 049 (43)	−6 999 (42)	1337 (61)	467 (36)	1052 (49)	9 (38)	931 (48)	−36 (33)
C12A	8 782 (103)	25 000 (0)	−6 973 (112)	552 (108)	777 (121)	598 (113)	0 (0)	349 (92)	0 (0)
C12B	2 877 (96)	25 000 (0)	−11 740 (83)	593 (102)	461 (81)	245 (71)	0 (0)	147 (72)	0 (0)
C13	35 485 (32)	14 674 (39)	74 208 (30)	538 (33)	547 (34)	401 (27)	−110 (28)	126 (26)	2 (24)
C14	43 555 (34)	10 204 (43)	77 676 (33)	589 (35)	561 (37)	513 (30)	−58 (31)	83 (27)	49 (27)
C15	45 833 (41)	1 812 (49)	83 839 (40)	706 (46)	686 (41)	737 (43)	−11 (37)	59 (37)	176 (35)
C16	40 195 (51)	−2 247 (61)	86 925 (46)	1060 (64)	1043 (58)	832 (49)	−178 (53)	74 (48)	512 (44)
C17	32 304 (49)	1 662 (65)	83 990 (50)	939 (61)	1291 (68)	998 (55)	−274 (53)	341 (49)	553 (50)
C18	30 020 (36)	10 219 (57)	77 650 (38)	615 (39)	1148 (58)	661 (37)	−55 (42)	198 (32)	284 (41)
C19	23 157 (45)	25 000 (0)	60 318 (45)	449 (47)	627 (48)	369 (40)	0 (0)	151 (37)	0 (0)
C20	18 769 (32)	15 690 (48)	56 497 (33)	499 (35)	934 (45)	475 (30)	−46 (34)	207 (28)	−19 (31)
C21	10 865 (35)	15 851 (59)	49 484 (37)	550 (40)	1352 (67)	570 (34)	−221 (42)	221 (33)	−215 (40)
C22	6 989 (51)	25 000 (0)	46 141 (55)	377 (53)	1696 (114)	483 (53)	0 (0)	131 (45)	0 (0)
C23	37 911 (43)	25 000 (0)	60 186 (43)	394 (42)	478 (41)	365 (38)	0 (0)	93 (34)	0 (0)
C24	39 831 (32)	15 697 (41)	56 638 (32)	527 (33)	572 (33)	489 (29)	59 (28)	153 (27)	−42 (26)
C25	43 665 (34)	15 736 (52)	50 418 (35)	520 (35)	1007 (51)	539 (32)	215 (36)	134 (30)	−88 (35)
C26	45 803 (48)	25 000 (0)	47 472 (55)	344 (49)	1392 (93)	549 (54)	0 (0)	162 (43)	0 (0)
C27	−26 937 (29)	14 550 (35)	70 412 (29)	452 (29)	451 (30)	393 (25)	56 (24)	177 (23)	−20 (22)
C28	−20 978 (31)	9 798 (42)	78 299 (32)	489 (31)	654 (37)	460 (28)	44 (29)	201 (26)	−19 (27)
C29	−22 735 (40)	1 099 (44)	82 650 (36)	790 (47)	616 (36)	530 (35)	226 (34)	322 (35)	197 (28)
C30	−30 647 (41)	−3 016 (43)	79 476 (39)	1006 (53)	484 (32)	689 (39)	43 (37)	553 (40)	103 (31)
C31	−36 742 (36)	1 573 (45)	72 019 (37)	649 (41)	660 (37)	620 (36)	−191 (33)	365 (33)	−135 (30)
C32	−34 974 (31)	10 268 (41)	67 633 (31)	491 (31)	591 (35)	480 (28)	−25 (28)	210 (25)	−13 (26)
C33	−15 255 (46)	25 000 (0)	65 720 (45)	499 (48)	453 (41)	424 (41)	0 (0)	161 (38)	0 (0)
C34	−11 021 (32)	15 653 (41)	65 530 (34)	544 (34)	560 (34)	604 (33)	41 (29)	269 (29)	59 (27)
C35	−3 112 (34)	15 599 (47)	65 349 (36)	637 (37)	706 (41)	643 (35)	202 (32)	311 (33)	63 (31)
C36	952 (49)	25 000 (0)	65 375 (53)	461 (53)	1060 (73)	555 (52)	0 (0)	231 (44)	0 (0)
C37	−30 666 (42)	25 000 (0)	53 954 (43)	390 (42)	429 (37)	405 (38)	0 (0)	166 (34)	0 (0)
C38	−32 860 (32)	15 674 (38)	48 764 (32)	541 (32)	459 (28)	471 (28)	−5 (26)	192 (26)	16 (24)
C39	−37 070 (35)	15 553 (41)	39 311 (33)	786 (41)	516 (31)	497 (31)	−103 (30)	288 (31)	−71 (26)
C40	−39 350 (53)	25 000 (0)	34 455 (48)	649 (58)	890 (63)	361 (43)	0 (0)	162 (42)	0 (0)
B1	33 015 (54)	25 000 (0)	67 251 (53)	451 (52)	476 (47)	375 (45)	0 (0)	119 (41)	0 (0)
B2	−24 971 (54)	25 000 (0)	65 280 (56)	463 (53)	394 (43)	474 (49)	0 (0)	168 (44)	0 (0)

atom	x	y	z	B,[c] Å^2	atom	x	y	z	B,[c] Å^2
CS1[d]	4100	2500	−99	10.00	H14C	−303	2500	−1471	5.00
CS2[d]	3300	2500	100	10.00	H14D	526	2500	−1625	5.00
NS1[d]	2700	2500	250	10.00	H15	4764	1313	7572	5.00
CS3[d]	3100	2500	−99	10.00	H16	5130	−111	8586	5.00
CS4[d]	4050	2500	150	10.00	H17	4178	−795	9122	5.00
NS2[d]	4700	2500	300	10.00	H18	2836	−125	8617	5.00
H1	−3610	936	−547	5.00	H19	2451	1303	7567	5.00
H2	−3260	1506	−1196	5.00	H20	2131	900	5878	5.00
H3	−3568	2500	176	5.00	H21	813	928	4701	5.00
H4	−4190	2500	−853	5.00	H22	153	2500	4144	5.00
H5	−1429	1054	4188	5.00	H23	3844	906	5858	5.00
H6	−2272	1286	3368	5.00	H24	4479	915	4814	5.00
H7	−1199	2500	4530	5.00	H25	4877	2500	4353	5.00
H8	−2169	2500	4138	5.00	H26	−1546	1266	8079	5.00
H9	2459	904	3401	5.00	H27	−1840	−201	8786	5.00
H10	2198	1543	4091	5.00	H28	−3186	−897	8245	5.00
H11	2267	2500	2527	5.00	H29	−4226	−121	6978	5.00
H12	3040	2500	3462	5.00	H30	−3939	1344	6255	5.00
H13A	96	1397	−1305	5.00	H31	−1366	903	6552	5.00
H13B	939	985	−576	5.00	H32	−45	902	6523	5.00
H13C	346	951	−1148	5.00	H33	642	2500	6536	5.00
H13D	1102	1486	−371	5.00	H34	−3136	907	5194	5.00
H14A	1008	2500	−1231	5.00	H35	−3840	895	3611	5.00
H14B	1380	2500	−155	5.00	H36	−4238	2500	2794	5.00

[a] Final value of the scale factor is 0.9565 (13). [b] The form of the anisotropic temperature factor is $\exp[-2\pi^2(h^2a^{*2}U_{11} + \ldots + 2klb^*c^*U_{23})]$. [c] Thermal parameters are of the form $\exp[-B(\sin^2\theta)/\lambda^2]$. [d] Positional occupancy = 0.5.

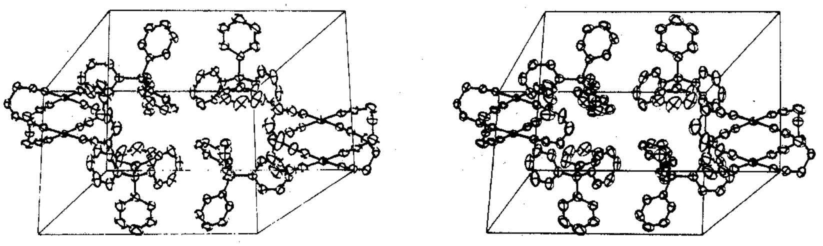

Figure 3. Stereoview of the $Rh_2(bridge)_4(BPh_4)_2 \cdot CH_3CN$ unit cell.

$\sigma^2(F_o^2)$, were based on counting statistics plus a term $(0.02P)^2$, where P is the scan count. Intensities and their weights ($w = 1/\sigma^2(F_o^2)$) were corrected for Lorentz and polarization effects but not for absorption ($\mu = 5.62$ cm^{-1}). The data were then placed on an absolute scale using Wilson's method and the scale factor was subsequently refined. Further crystal data are given in Table I.

Structure Determination The structure was solved by the heavy-atom method and refined by using blocked matrix least-squares techniques. Approximate coordinates for the Rh atom were obtained from a sharpened Patterson map. A series of structure factor and difference map calculations revealed all the remaining nonhydrogen atoms except for the disordered acetonitrile molecule (vide infra). The initial agreement factor $R_F = \sum||F_o| - |F_c||/\sum|F_o|$ was 0.28.

Isotropic refinement was initiated by using atomic scattering factors from Cromer and Waber[12] for Rh, and from ref 13 for C, N, and B. Hydrogen scattering factors were obtained from Stewart et al.[14] Both real and imaginary parts of the anomalous dispersion correction were applied to Rh. Several cycles of refinement (quantity minimized was $\sum w(F_o^2 - (1/s^2)F_c^2)^2$, $w = 1/\sigma^2(F_o^2)$, s = scale factor) resulted in isotropic convergence at $R_F = 0.12$. At this point it was noted that C12 had an unusually large thermal parameter ($B \geq 10$). Examination of difference maps revealed the presence of a peak near C12 and thus suggested a disorder. The population of C12 in the two positions (C12A, C12B) was equally partitioned. Several peaks of moderate intensity at $y = {}^1/_4$ were also noted and ascribed to a disordered CH_3CN molecule. Neither occupancy, positional, nor thermal parameters were refined.

Further refinement was carried out by using anisotropic thermal parameters for the nonhydrogen atoms. Due to the large number of parameters (418), the refinement was blocked into two matrices with the scale factors and thermal parameters in one and the coordinates in the other. Several cycles of refinement reduced R_F to 0.09. Idealized hydrogen positions were calculated (C–H = 0.95 Å) and found to correspond to areas of positive electron density in a difference map calculated at this point. An isotropic thermal parameter of 5.0 Å^2 was assigned to all hydrogens. Additional blocked matrix refinement cycles converged at $R_F = 0.048$ (R_F based on all data with $F > 0$ was 0.12). On the last cycle all positional and thermal parameter changes were within their estimated standard deviation. The final "goodness of fit" $((\sum w(F_o^2 - F_c^2)/(m - s))^{1/2}$ where m is the number of observations and s is the number of parameters varied) was 1.98. A final difference Fourier map showed a general background of approximately 0.3 e/Å^3 and no peaks larger than 0.8 e/Å^3. Final atomic parameters are given in Table II. A list of observed and calculated structure factors is available in Supplementary Table 1.

The structure consists of discrete tetraphenylborate anions and binuclear cations having m symmetry with the mirror (at $y = {}^1/_4$) perpendicular to the Rh–Rh axis. The mirror passes through C3, C6, C9, and C12 (A, B). There are no close contacts between binuclear units. Shown in Figures 1–3 are a perspective view of the complex, a molecular packing diagram, and a stereoview of the unit cell. Important bond distances and angles are given in Table III.

The Rh–Rh distance is 3.242 (1) Å; each Rh atom is coordinated by four isocyanide ligands in effectively square-planar geometry, the entire cation having approximate D_{4h} symmetry.

The tetraphenylborate anions, which also have symmetry m, are completely unexceptional. There are no short intermolecular contact distances between the binuclear cations and anions or solvent molecules.

Table III. Bond Distances (Å) and Angles (Deg)[a] for $Rh_2(bridge)_4(BPh_4)_2 \cdot CH_3CN$

Cation Distances			
Rh-Rh	3.242 (1)		
Rh-C1	1.959 (4)	Rh-C7	1.976 (4)
Rh-C4	1.960 (4)	Rh-C10	1.960 (4)
C1-N1	1.128 (5)	N1-C2	1.434 (7)
C4-N2	1.144 (6)	N2-C5	1.455 (7)
C7-N3	1.147 (5)	N3-C8	1.443 (5)
C10-N4	1.146 (5)	N4-C11	1.452 (6)
C2-C3	1.147 (8)	C8-C9	1.515 (5)
C5-C6	1.357 (9)	C11-C12A	1.402 (10)
		C11-C12B	1.429 (8)
Cation Angles			
Rh-C1-N1	176.3 (4)	Rh-C4-N2	175.5 (4)
Rh-C7-N3	174.9 (4)	Rh-C10-N4	175.4 (4)
C1-Rh-C4	88.3 (2)	C1-Rh-C7	177.6 (2)
C1-Rh-C10	91.3 (2)	C4-Rh-C10	177.9 (2)
C4-Rh-C7	92.4 (2)	C7-Rh-C10	87.9 (2)
C1-N1-C2	174.4 (5)	C7-N3-C8	174.7 (4)
N1-C2-C3	113.0 (5)	N3-C8-C9	110.9 (3)
C2-C3-C2M[b]	119.7 (5)	C8-C9-C8M	114.8 (3)
C4-N2-C5	174.0 (5)	C10-N4-C11	175.6 (4)
N2-C5-C6	118.0 (6)	N4-C11-C12A	118.0 (5)
C5-C6-C5M	137.2 (6)	N4-C11-C12B	112.8 (5)
C11-C12A-C11M	126.4 (7)	C11-C12B-C11M	122.2 (6)
Average[c] Tetraphenylborate Distances			
C-C	1.38 (2)	C-B	1.65 (1)
Average Tetraphenylborate Angles			
B-C-C	122.5 (4)	C-C-C	120 (2)
C-B-C	112 (9)		

[a] Estimated standard deviations in parentheses. Atom coordinate esd's are made isotropic by averaging orthonormalized esd's. No correlation effects have been accounted for. [b] M refers to atom related by x, ${}^1/_2 - y$, z. [c] The standard deviation given in parentheses following an average bond distance or angle, $\bar{x}$, is defined as $\sigma = [\Sigma_i(x_i - \bar{x})^2/(N-1)]^{1/2}$, where N is the number of observations, x_i.

Collection and Data Reduction for $Rh_2(TM4\text{-}bridge)_4(PF_6)_2 \cdot 2CH_3CN$. Crystals were grown by layering diethyl ether above a concentrated acetonitrile solution of $Rh_2(TM4\text{-}bridge)_4(PF_6)_2$. A crystal (0.18 × 0.42 × 0.34 mm) was mounted in a glass capillary along its long dimension to limit powdering, presumably from solvent loss. Precession photographs indicated $4/mmm$ symmetry with the systematic absences $0kl$, $k = 2n + 1$, hhl, $l = 2n + 1$, which suggested either space group $P4_2bc$ or $P4_2/mbc$; the latter gave a successful solution. Unit cell constants were obtained from a least-squares fit of 15 centered reflections. The density, 1.29 (1) g/cm^3, measured by the flotation method in a mixture of carbon tetrachloride and toluene, is in reasonable agreement with the calculated value of 1.294 (1) g/cm^3 on the basis of four formula units per unit cell.

Intensity data were collected at room temperature (22 °C) on a Syntex $P2_1$ automated full-circle diffractometer using graphite monochromatized Mo Kα radiation. The θ–2θ scan method was used on the octant $+h,+k,+l$ from 2θ = 0–50°. Each scan ranged from 0.9° below Kα_1 to 0.9° above Kα_2 for the calculated peak position at a rate of 2.02° min^{-1}. Stationary-background counts, each of which equaled half of the scan time, were taken before and after each scan. Crystal decomposition was monitored by five standard check re-

---

[12] Cromer, D. T.; Waber, J. T. *Acta Crystallogr.* **1965**, *18*, 104.

[13] "International Tables for X-ray Crystallography"; Kynoch Press: Birmingham, England, 1962; Vol. III.

[14] Stewart, R. F.; Davidson, E. R.; Simpson, W. T. *J. Chem. Phys.* **1965**, *42*, 3175.

Table IV. Final Atom Parameters (Coordinates × 10^5, U_{ij} × 10^4)[a,b] for $Rh_2(TM4\text{-bridge})_4(PF_6)_2 \cdot 2CH_3CN$

atom	x	y	z	U_{11}	U_{22}	U_{33}	U_{12}	U_{13}	U_{23}
Rh	−7 851 (5)	42 148 (5)	25 000 (0)	367 (2)	367 (2)	557 (7)	48 (7)	207 (4)	207 (4)
C2	1 240 (70)	32 714 (70)	23 352 (33)	361 (65)	377 (65)	645 (87)	−37 (54)	24 (55)	−13 (57)
N2	6 821 (66)	27 673 (59)	22 175 (32)	563 (69)	357 (57)	818 (71)	158 (55)	59 (63)	−92 (53)
C3	14 480 (90)	21 948 (83)	20 688 (47)	793 (109)	528 (94)	899 (109)	377 (78)	229 (90)	16 (83)
CME1	13 028 (90)	12 816 (88)	22 661 (52)	607 (94)	483 (86)	1756 (174)	44 (80)	−79 (96)	−218 (93)
CME2	14 051 (97)	21 548 (99)	15 618 (54)	884 (118)	946 (128)	1056 (121)	239 (96)	193 (104)	−219 (107)
C4	23 110 (103)	26 667 (112)	22 432 (31)	364 (119)	563 (134)	1036 (82)	81 (52)	98 (122)	−159 (135)
C1	−6 446 (66)	39 819 (57)	31 394 (36)	377 (72)	221 (60)	617 (70)	−50 (48)	−14 (63)	−10 (52)
N1	−6 156 (65)	38 862 (60)	35 303 (33)	657 (75)	565 (63)	623 (65)	−59 (54)	+64 (63)	−36 (55)
C5	−5 966 (145)	38 919 (110)	40 242 (48)	2666 (281)	975 (141)	643 (96)	−822 (178)	−18 (139)	−220 (96)
CME3	−1 934 (192)	30 518 (144)	41 800 (67)	4117 (393)	1744 (232)	1647 (209)	−1909 (256)	+1888 (248)	−831 (178)
CME4	−15 770 (225)	37 796 (119)	41 817 (70)	5527 (525)	616 (130)	1826 (214)	−706 (225)	−1831 (282)	127 (143)
C6	3 953 (115)	47 986 (168)	41 664 (40)	1397 (214)	2525 (240)	692 (92)	358 (175)	−339 (111)	−489 (158)
P	13 727 (46)	23 482 (52)	0 (0)	899 (50)	1093 (56)	758 (47)	375 (0)	0 (0)	0 (0)
F1	4 211 (109)	25 583 (169)	0 (0)	1160 (141)	3352 (274)	3087 (256)	899 (0)	0 (0)	0 (0)
F2	14 661 (156)	33 512 (132)	0 (0)	2521 (277)	1531 (193)	3568 (300)	−176 (0)	0 (0)	0 (0)
F3	23 745 (106)	22 494 (145)	0 (0)	999 (125)	3145 (265)	2708 (204)	380 (0)	0 (0)	0 (0)
F4	13 630 (182)	14 017 (115)	0 (0)	3719 (358)	806 (127)	4884 (461)	−370 (0)	0 (0)	0 (0)
F56	14 107 (105)	23 882 (112)	4 853 (33)	3875 (237)	3469 (220)	792 (78)	1644 (187)	172 (105)	349 (122)

atom	x	y	z	B,[c] Å^2	atom	x	y	z	B,[c] Å^2
C10[d]	4007 (16)	4122 (17)	1081 (9)	5.00	HM23	990	2626	1409	6.00
N10[d]	3811 (13)	3962 (14)	1450 (7)	5.00	HM31	5008	1984	4512	6.00
CME5[d]	3983 (18)	3994 (18)	613 (9)	6.00	HM32	4418	2529	4126	6.00
HC4A	2379	3360	2142	6.00	HM33	5429	2101	3973	6.00
HC4B	2937	2399	2126	6.00	HM41	3190	1850	4201	6.00
HM11	1090	1287	2622	6.00	HM42	3364	943	4521	6.00
HM12	1809	821	2276	6.00	HM43	3037	796	3983	6.00
HM13	758	944	2113	6.00	HM51	4465	3574	515	6.00
HM21	1160	1521	1442	6.00	HM52	4193	4709	507	6.00
HM22	2008	2195	1383	6.00	HM53	3366	3926	452	6.00

[a] Final value of the scale factor is 0.207 (3). [b] The form the anisotropic temperature factor is $\exp[-2\pi^2(h^2a^{*2}U_{11} + \ldots + 2klb^*c^*U_{23})]$. [c] Thermal parameters are of the form $\exp[-B(\sin^2\theta)/\lambda^2]$. [d] Positional occupancy = 0.5.

Table V. Bond Distances (Å) and Angles (Deg)[a] for $Rh_2(TM4\text{-bridge})_4(PF_6)_2 \cdot 2CH_3CN$

Cation Distances

Rh-Rh	3.262 (1)		
Rh-C1	1.92 (1)	Rh-C2	1.98 (1)
C1-N1	1.16 (1)	C2-N2	1.16 (1)
N1-C5	1.45 (2)	N2-C3	1.47 (2)
C3-C4	1.53 (2)	C5-C6	2.02 (2)
C4-C4′	1.51 (3)	C6-C6′	1.30 (3)
C3-CME1	1.48 (3)	C5-CME3	1.44 (3)
C3-CME2	1.49 (2)	C5-CME4	1.52 (3)

Cation Angles

C1-Rh-C2	92.4 (4)		
Rh-C1-N1	175 (1)	Rh-C2-N2	175 (1)
C3-N2-C2	175 (1)	C1-N1-C5	173 (1)
N1-C5-C6	103 (1)	N2-C3-C4	106 (1)
C5-C6-C6′	72 (1)	C3-C4-C4′	111 (5)
N1-C5-CME3	109 (1)	N2-C3-CME1	107 (5)
N1-C5-CME4	107 (1)	N2-C3-CME2	107 (1)
C6-C5-CME3	102 (1)	C4-C3-CME1	114 (5)
C6-C5-CME4	134 (1)	C4-C3-CME2	113 (1)
CME3-C5-CME4	102 (2)	CME1-C3-CME2	110 (5)

Anion Distances

P-F1	1.43 (2)	P-F4	1.39 (2)
P-F2	1.48 (2)	P-F56	1.43 (2)
P-F3	1.48 (2)		

Anion Angles

F1-P-F2	83 (1)	F56-P-F56	173 (1)
F1-P-F3	173 (1)	F56-P-F1	92 (1)
F1-P-F4	102 (1)	F56-P-F2	87 (1)
F2-P-F3	90 (1)	F56-P-F3	88 (1)
F2-P-F4	175 (1)	F56-P-F4	92 (1)
F3-P-F4	85 (1)		

Disordered Acetonitrile Distances

C10-N10	1.15 (3)	C10-CME5	1.39 (3)

Disordered Acetonitrile Angles

N10-C10-CME5	155 (2)

[a] Estimated standard deviations in parentheses. Atom coordinate esd's are made isotropic by averaging orthonormalized esd's. No correlation effects have been accounted for.

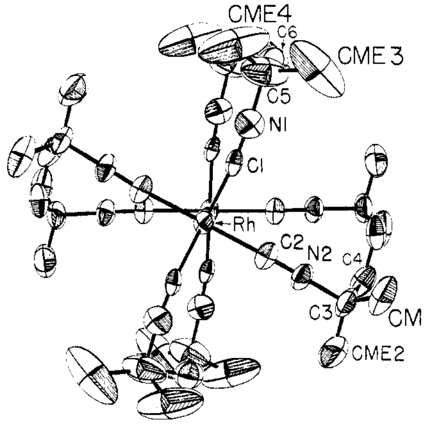

Figure 4. View of the structure of $Rh_2(TM4\text{-bridge})_4^{2+}$.

flections, which were collected every 95 reflections. No significant decay or fluctuations (±2%) were observed in any of the check reflections during the 170 h of data collection. After averaging *hkl* with *khl*, the entire data set consisted of 2893 independent reflections of which 1283 had $F_o^2 > 3\sigma(F_o^2)$. For 881 reflections, background counts were affected by overlap from neighboring reflections (due to the length of the *c* axis); the intensities of these reflections and four others that were partially blocked by the beam stop were given zero weight in the refinement.

The remaining data (2008) were corrected for Lorentz and polarization effects. Observational variances, $\sigma^2(F_o)^2$, were based on counting statistics plus the term $(0.02P)^2$, where P is the scan count. No correction was made for absorption ($\mu = 6.29$ cm^{-1}). Data were placed on an absolute scale by Wilson's method and the scale factor was subsequently refined. Additional crystal data are given in Table I.

Structure Determination. A Patterson synthesis gave approximate coordinates for the Rh atom and subsequent Fourier and difference Fourier maps yielded all nonhydrogen atoms except a partially occupied acetonitrile. The initial agreement factor, $R = \sum||F_o| - |F_c||/\sum|F_o|$, was 0.34.

Again, scattering factors for Rh were from Cromer and Waber,[12] those for C, N, P, and F from ref 13, and those for hydrogen from

Table VI. Absorption Spectral Data[a] for Rhodium Complexes

complex	$^1A_{1g} \rightarrow {}^1E_u$	$^1A_{1g} \rightarrow {}^3E_u$	not assigned	$^1A_{1g} \rightarrow {}^1A_{2u}$	$^1A_{1g} \rightarrow {}^3A_{2u}$
Rh(CN-*t*-Bu)$_4^+$ [b]	310 (25.5)	335 (3.40)	*c*	386 (9.90)	442 (0.30)
Rh(CNPh)$_4^+$	335 (49.1)	*c*	*c*	411 (5.94)	462 (0.67)
Rh$_2$(CN-*t*-Bu)$_8^{2+}$	*c*	*c*	*c*	490 (16.9)	*c*
Rh$_2$(bridge)$_4^{2+}$	318 (31.5)	344 (5.5)	380 (*d*)	553 (14.5)	*c*
Rh$_2$(4-bridge)$_4^{2+}$	313 (37.3)	334 (5.0) sh	380 (0.8)	526 (10.9)	*c*
Rh$_2$(TM4-bridge)$_4^{2+}$	313 (43.3)	338 (3.9)	390 (0.5)	515 (11.7)	*c*

[a] Band positions in nm; $\epsilon \times 10^{-3}$ values in parentheses. [b] Measured in aqueous solution at 25 °C; all other spectra were recorded in CH_3CN solution at 25 °C. [c] Not observed. [d] Not measured.

Table VII. Emission Spectral Data for Binuclear Rhodium Complexes

complex	emission max[a]	half-width, cm^{-1}	quantum yield	stokes shift, cm^{-1}
Rh$_2$(CNPhCH$_3$)$_8^{2+}$	697 (14 350)[b,c]	1940	0.0065[d]	3450
Rh$_2$(bridge)$_4^{2+}$	656 (15 240)[b]	1580	0.056[d]	2840
Rh$_2$(4-bridge)$_4^{2+}$	634 (15 770)	1830	0.077[e]	3240
Rh$_2$(TM4-bridge)$_4^{2+}$	614 (16 260)	1810	0.046	3160

[a] Band positions in nm; cm^{-1} in parentheses; $\lambda_{ex} = 505$ nm unless noted otherwise; all measurements were made in CH_3CN solution at 25 °C. [b] The emission lifetime is less than 2 ns. [c] $\lambda_{ex} =$ 510 nm. [d] Relative to Ru(bpy)$_3^{2+}$; see ref 5. [e] Relative to Rh$_2$(bridge)$_4^{2+}$.

Stewart et al.[14] The quantity minimized in the least-squares calculations was $\sum w[F_o^2 - (1/s^2)(F_c^2)]^2$, where $w = 1/\sigma^2(F_o^2)$ and $s =$ scale factor. Anisotropic refinement of all nonhydrogen atoms converged at an R index of 0.15. The addition of hydrogens (C–H = 0.95 Å) and a partially occupied acetonitrile, suggested by a difference Fourier map, yielded $R = 0.11$. Further refinement (blocked into two matrices: thermal parameters and scale factor in one, coordinates in another) of the nonhydrogen atoms was restricted to data in which $I > 3\sigma$ (=1283 reflections). This yielded convergence at $R = 0.078$ with a "goodness of fit" of 2.58 ($[\sum(F_o^2 - F_c^2)^2/(m - s)]^{1/2}$, where m = number of reflections and s = number of parameters). On the final cycle of least squares all positional and thermal parameter changes were within their estimated standard deviations. The final R index was 0.119 and the goodness of fit was 2.77. The final positional and thermal parameters are given in Table IV.

One difficulty encountered was apparent disorder in the position of C6. Least-squares refinement repeatedly shifted C6 toward the twofold axis, yielding a long C5–C6 bond, 2.018 (24) Å, and a short C6–C6′ bond, 1.303 (25) Å. A fit to two half-occupied C6 positions was attempted, but the refinement was not successful. A list of observed and calculated structure factors is available in Supplementary Table 2.

The structure consists of the binuclear cations, hexafluorophosphate anions, and acetonitrile molecules. A view of the cation is shown in Figure 4. Important bond distances and angles are listed in Table V. The center of the binuclear cation lies at a crystallographic special position that requires D_2 symmetry. The rhodium atoms are bridged (Rh–Rh = 3.262 (1) Å) by four TM4-bridge ligands that are arranged as a four-bladed propeller about the Rh–Rh axis, giving the two Rh(CN)$_4$ units a partially staggered conformation. The two torsional angles defined by N1–Rh–Rh′–N1′ and N2–Rh–Rh′–N2′ are identical within experimental error (31.0 (1) and 30.7 (1)°, respectively). The pitch of the blade is 32.0 (1)°, as measured from C3–Rh–Rh′–C3′. In light of the large thermal parameters and apparent disorder present, we feel that the dimensions associated with atoms C5, C6, C5′, and C6′ are virtually meaningless.

The hexafluorophosphate anion has the expected octahedral geometry. The average P–F bond distance (1.44 Å) is within the rather wide range of values (1.39–1.48 Å) found[15] in other determinations. While there is no evidence of disorder, the F atoms show large thermal motions in directions perpendicular to the P–F bonds. The parameters associated with the acetonitrile molecule are poorly defined due to partial occupancy (0.5). The C≡N distance of 1.15 (3) Å is as expected but the C–C bond of 1.39 (3) Å and C–N–C angle of 155 (2)° are far from the values normally found.

Structural Comparisons

The fact that the Rh–Rh distance is nearly the same in the two bridged binuclear Rh(I) complexes suggests that the Rh–Rh bonding interactions are not affected appreciably by changes in the relative rotameric conformation of the two Rh(CN)$_4$ planes. This result is reasonable, since even in the fully eclipsed conformations the ligand–ligand interactions should be relatively small. A best fit plane of the Rh(CN)$_4$ units (Supplementary Table 3) shows that in each complex there are very slight distortions. Each Rh in Rh$_2$(bridge)$_4^{2+}$ experiences a pyramidal distortion in which all four CN groups are displaced slightly toward the center of the cation. In Rh$_2$(TM4-bridge)$_4^{2+}$, on the other hand, the coordination about each Rh is tetrahedrally distorted in a manner similar to that observed[2] for Rh$_2$(CNPh)$_8$(BPh$_4$)$_2$. The bond distances and angles associated with the immediate coordination sphere of the Rh atom in both binuclear complexes are within the ranges observed in other known Rh(I) isocyanide complexes. The average Rh–C distances for both binuclear cations of 1.96 Å are comparable to those reported for Rh^{I}(fumaronitrile)(P(OC$_6$H$_5$)$_3$)(p-CH$_3$OC$_6$H$_4$NC)$_2$ (1.96 Å)[16] and Rh$_2$(CNPh)$_8$(BPh$_4$)$_2$ (1.94 Å).[2] Other average bond lengths in the two complexes are C≡N (1.14 (1) Å, bridge; 1.16 (1) Å, TM4-bridge), N—C (1.45 (1) Å, bridge; 1.46 (1) Å, TM4-bridge), C—C (1.43 (6) Å, bridge; 1.52 (2) Å, TM4-bridge), and C-Me (1.48 (4) Å, TM4-bridge). The average Rh-C-N angles of 175° and the C-N-C angles of 174° are close to 180°, comparing favorably with the values found[2] in Rh$_2$(CNPh)$_8$(BPh$_4$)$_2$. While the distances and angles found for the TM4-bridge complex in the C2–N2–C3–C4 chain are normal for such bonds, the disorder encountered at C6 (as previously discussed) may contribute to the deviations (±0.02 Å) noted in some of the C1–N1–C5–C6 bonds. C6 may be placed at a reasonable position, but upon refinement it shifts toward its related position about the twofold axis passing through the chain. This has the apparent effect of shortening the C6–C6′ distance and elongating C5–C6 to an unreasonable value.

Electronic Spectra

It is now well established that a principal electronic spectroscopic feature of binuclear rhodium(I) isocyanide complexes (with Rh–Rh in the range 3.19–3.26 Å) is a prominent low-lying absorption band attributable to $^1A_{1g} \rightarrow {}^1A_{2u}$ ($1a_{2u} \rightarrow 2a_{1g}$).[1-3,17-19] The position of the $^1A_{1g} \rightarrow {}^1A_{2u}$ band is a function of the rotameric conformation of the CNR groups, as shown by comparison of eclipsed (Rh$_2$(bridge)$_4^{2+}$) and partially staggered (Rh$_2$(TM4-bridge)$_4^{2+}$) complexes in which

---

(15) Goldberg, S. Z.; Eisenberg, R.; Miller, J. S. *Inorg. Chem.* **1977**, *16*, 1502 and references therein.

(16) Gaughan, A. P., Jr.; Ibers, J. A. *Inorg. Chem.* **1975**, *14*, 3073.

(17) Endres, H.; Gottstein, N.; Keller, H. J.; Martin, R.; Rodemer, W.; Steiger, W. *Z. Naturforsch., B* **1979**, *34*, 827.

(18) Kawakami, K.; Okajima, M.; Tanaka, T. *Bull. Chem. Soc. Jpn.* **1978**, *51*, 2327.

(19) Yaneff, P. V.; Powell, J. *J. Organomet. Chem.* **1979**, *179*, 101.

the Rh–Rh distance is about the same (Table VI). Whether the observed transition energy differences are due mainly to the nature of the distortions at each Rh atom or are attributable to interunit (CNR···CNR) interactions, or some combination of effects, cannot be determined without further study.

Additional evidence that the rotameric conformation influences the relative energy of the $^1A_{2u}$ excited state of these binuclear rhodium(I) isocyanide complexes comes from studies of their emission spectra in fluid solution (Table VII). The relatively high emission quantum yields and short lifetimes (<2 ns) suggest that the emission originates from the same excited state reached in absorption; i.e., the transition is $^1A_{2u} \rightarrow {}^1A_{1g}$. It is interesting that the largest Stokes shifts are observed for the complexes with staggered ground-state conformations, the order being $CNPhCH_3$ (staggered)[20] > 4-bridge ~ TM4-bridge (partially staggered) > bridge (eclipsed). The half-widths of the emission bands also follow the same order.

The intense bands at 318 nm for $Rh_2(bridge)_4^{2+}$ and at 313 nm for $Rh_2(TM4\text{-}bridge)_4^{2+}$ and $Rh_2(4\text{-}bridge)_4^{2+}$ are assigned to the fully allowed $^1A_{1g} \rightarrow {}^1E_u$ ($d_{xz},d_{yz} \rightarrow \pi^*$ CNR) transition. The fact that the position of this band in the various binuclear Rh(I) complexes is close to that in a related monomer (310 nm in $Rh(CN\text{-}t\text{-}Bu)_4^+$) suggests that the d_{xz},d_{yz} orbitals on one Rh atom do not interact significantly with those on the other Rh atom. The corresponding singlet–triplet transition, $^1A_{1g} \rightarrow {}^3E_u$, occurs at about 340 nm in the spectrum of each complex. Assignment of this band also follows from the interpretation of the spectrum of $Rh(CNEt)_4^+$ given previously by Isci and Mason.[21]

Acknowledgment. We thank Richard Marsh, Wayne Gladfelter, and Andrew Maverick for many helpful discussions. This research was supported by National Science Foundation Grant No. CHE78-10530. The X-ray instrumentation was obtained with the aid of NSF Instrument Grant No. CHE76-05471.

Registry No. $Rh_2(bridge)_4(BPh_4)_2 \cdot CH_3CN$, 73367-40-5; $Rh_2(TM4\text{-}bridge)_4(PF_6)_2 \cdot 2CH_3CN$, 73367-43-8; $[Rh(COD)Cl]_2$, 12092-47-6; $Rh_2(CO)_4Cl_2$, 14523-22-9; $Rh(CN\text{-}t\text{-}Bu)_4^+$, 34195-61-4; $Rh(CNPh)_4^+$, 56192-48-4; $Rh_2(CN\text{-}t\text{-}Bu)_8^{2+}$, 73367-44-9; $Rh_2(4\text{-}bridge)_4^{2+}$, 67783-56-6; $Rh_2(CNPhMe)_8^{2+}$, 65918-76-5.

Supplementary Material Available: Listings of observed and calculated structure factor amplitudes and best fit planes (30 pages). Ordering information is given on any current masthead page.

---

[20] It is reasonable to assume that the ground-state structure of $Rh_2(CNPhCH_3)_8^{2+}$ does not differ significantly from that of $Rh_2(CNPh)_8^{2+}$, the latter possessing a staggered CNPh–CNPh rotameric conformation.[2]

[21] Isci, H.; Mason, W. R. *Inorg. Chem.* **1975**, 14, 913.

Notes

Contribution from the Departments of Chemistry,
Washington State University, Pullman, Washington 99163,
and Third College, University of California, San Diego,
La Jolla, California 92093

Stereochemistry of the Photolysis of *trans*-$Cr(en)_2F_2^+$

Steven C. Pyke and Robert G. Linck*

Received July 20, 1978

The stereochemical consequences upon photoaquation of Cr(III) complexes have been a central theme of such studies,[1,2] perhaps only slightly less important than the issue of models to identify the leaving group.[3–7] Especially important in this area are the careful experiments of Kirk and co-workers[8,9] on a variety of Cr(III) complexes in which "stereomobility"—a net change in stereochemistry upon photoaquation—is generally observed. However, a number of reactions have been reported in which the net stereochemistry of the reaction is retentive.[6,10–12] (The difference between the apparent and mechanistic stereochemical inversion is discussed by Walters and Linck.[12]) This conclusion was first demonstrated by Pyke and Linck,[10] who claimed the major photoproduct of *trans*-$Cr(en)_2F_2^+$ was the isomer of $Cr(en)(enH)(H_2O)F_2^{2+}$ produced from thermal aquation[13] of *trans*-$Cr(en)_2F_2^+$, presumably **1**. With two recent developments the subject of lack of apparent stereomobility, especially in *trans*-$Cr(en)_2F_2^+$, has taken on added importance. These are (1) a theoretical treatment of the stereomobility in Cr(III) complexes,[14] even a specific discussion of the role of fluoride[15] in affecting stereochemistry, and (2) a report indicating that the products of photoaquation on *trans*-$Cr(en)_2F_2^+$ are substantially[16] different from **1**. In this note we reexamine the products of photoaquation of *trans*-$Cr(en)_2F_2^+$ to establish the stereochemical consequences.

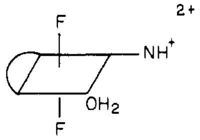

1

Experimental Section

[*trans*-$Cr(en)_2F_2$]ClO_4 was prepared and purified as described previously.[13] Photolysis was carried out either under broad-band (λ >400 nm) irradiation or through a 520-nm interference filter (the latter for quantum yield experiments). The apparatus used has been described.[10] Actinometry was based on Wegner and Adamson's

---

* To whom correspondence should be addressed at the Third College, University of California, San Diego.

[1] V. Balzani and V. Carassiti, "Photochemistry of Coordination Compounds", Academic Press, New York, 1970.
[2] E. Zinato in "Concepts of Inorganic Chemistry", A. W. Adamson and P. D. Fleischauer, Ed., Wiley, New York, 1975, pp 143–201.
[3] A. W. Adamson, *J. Phys. Chem.*, **71**, 798 (1967).
[4] J. I. Zink, *J. Am. Chem. Soc.*, **94**, 8039 (1972).
[5] M. Wrighton, H. B. Gray, and G. S. Hammond, *Mol. Photochem.*, **5**, 165 (1973).
[6] C. Bifano and R. G. Linck, *Inorg. Chem.*, **13**, 609 (1974).
[7] L. G. Vanquickenborne and A. Ceulemans, *J. Am. Chem. Soc.*, **99** 2208 (1977).
[8] A. D. Kirk, *Inorg. Chem.*, **18**, 2326 (1979).
[9] A. D. Kirk and C. F. C. Wong, *Inorg. Chem.*, **18**, 593 (1979), and references therein.
[10] S. C. Pyke and R. G. Linck, *J. Am. Chem. Soc.*, **93** 5281 (1971).
[11] G. Wirth and R. G. Linck, *J. Am. Chem. Soc.*, **95**, 5913 (1973).
[12] R. T. Walters and R. G. Linck, *Inorg. Chem.*, **14**, 2098 (1975).
[13] S. C. Pyke and R. G. Linck, *Inorg. Chem.*, **10**, 2445 (1971).
[14] L. G. Vanquickenborne and A. Ceulemans, *J. Am. Chem. Soc.*, **100**, 475 (1978).
[15] L. G. Vanquickenborne and A. Ceulemans, *Inorg. Chem.*, **18**, 3475 (1979).
[16] M. F. Manfrin, D. Sandrini, A. Juris, and M. T. Gandolfi, *Inorg. Chem.*, **17**, 90 (1978).

0020-1669/80/1319-2468$01.00/0